Optical absorption and fluorescence spectroscopy studies of Artepillin C, the major component of green propolis

Isamara Julia Camuri [a], Adriano Batista Costa [a], Amando Siuiti Ito [a], Wallance Moreira Pazin [b],*

[a] Department of Physics, Faculty of Philosophy, Sciences and Letters of Ribeirão Preto, University of São Paulo (USP), Ribeirão Preto, SP, Brazil
[b] Department of Physics, School of Sciences and Technology, São Paulo State University (UNESP), Presidente Prudente, SP, Brazil

ABSTRACT

The bioactivity of propolis against several pathogens is well established, leading to the extensive consumption of that bee product to prevent diseases. Brazilian green propolis, collected by the species *Apis mellifera*, is one of the most consumed in the world. The chemical composition of green propolis is complex and it has been shown that it displays antioxidant, antimicrobial, anti-inflammatory and antitumor activities, especially due to the high content of Artepillin C. The molecule is a derivative of cinnamic acid with two prenylated groups, responsible for the improvement of the affinity of the compound for lipophilic environment. A carboxylic group (COOH) is also present in the molecule, making it a pH-sensitive compound and the pH-dependent structure of Artepillin C, may modulate its biological activity related to interactions with the cellular membrane of organisms and tissues. Molecular properties of Artepillin C on aqueous solution were examined by optical absorption, steady state and time-resolved fluorescence spectroscopies. Acid-base titration based on the spectral position of the near UV absorption band, resulted in the pKa value of 4.65 for the carboxylic group in Artepillin C. In acidic pH, below the pKa value, an absorption band raised around 350 nm at Artepillin C concentration above 50 μM, due to aggregation of the molecule. In neutral pH, with excitation at 310 nm, Artepillin C presents dual emission at 400 and 450 nm. In pH close to the pKa, the optical spectra show contribution from both protonated and deprotonated species. A three-exponential function was necessary to fit the intensity decays at the different pHs, dominated by a very short lifetime component, around 0.060 ns. The fast decay resulted in emission before fluorescence depolarization, and in values of fluorescence anisotropy higher than could be expected for monomeric forms of the compound. The results give fundamental knowledge about the protonation-deprotonation state of the molecule, that may be relevant in processes mediated by biological membranes.

© 2018 Elsevier B.V. All rights reserved.

1. Introduction

The protection of beehives against intruders is guaranteed by the plant resins collected by the bees to produce the propolis, that, in Greek, means "*pro* = in defense" and "*polis* = city" [1]. The final product is constituted mainly by the mixture of the resinous compounds and beeswax, enabling bees to seal their nests for the asepsis [2]. Ancient civilization took advantage of the biological properties of propolis to be used in folk medicine, for instance as anti-pyretic, antiseptic and cicatrizing agent [3]. Since then, propolis has been extensively consumed in food and beverages until nowadays as a popular remedy to prevent diseases and act against several pathogens, mainly due to its established antimicrobial properties [4].

The chemical composition of propolis is complex and dependent on the region that bees can access to collect the resinous compounds, but it is known that bees search for secondary metabolites synthetized by the plant enzymes to ensure its biological protection [5]. In European countries and China, for instance, the major constituents of propolis are several classes of flavonoids and phenolic acid esters, while in Brazil, besides the presence of flavonoids, most of propolis is constituted mainly by terpenoids and prenylated derivatives of *p*-coumaric acid [6,7]. Among all Brazilian propolis, the green propolis, processed by bee species *Apis mellifera*, is one of the most consumed propolis in the world, mainly in Japan [8]. It has been shown that this propolis displays antioxidant, antimicrobial, anti-inflammatory and antitumor activities, especially due to the high amount of Artepillin C, a cinnamic acid derivative that presents two prenylated groups (Fig. 1), responsible to improve the affinity of the compound for lipophilic environment, for instance biological membranes, in the biological action in target cells [3,9–12].

Artepillin C also present the carboxylic acid group (COOH), bringing it to a particular class of pH-sensitive compounds. It has been established that, due to the differences in the molecular structure of such compounds dependent on the pH of the medium, they might be

* Corresponding author at: Departamento de Física, FCT – UNESP, Presidente Prudente, SP, Rua Roberto Simonsen, 305, 19060-900 Presidente Prudente, São Paulo, Brazil.
E-mail address: wallancepazin@gmail.com (W.M. Pazin).

selective in their biological actions [13]. A correlation between biological properties of Artepillin C and its particular structure may exist: it is thought that the compound, in healthy physiological conditions, improves the antioxidant potential of the biological system via one-step hydrogen atom transfer mostly by interacting with cell membranes, probably due to the presence of prenylated groups, avoiding the formation of lipid peroxidation caused by free radicals that damage membrane structure with low toxicity [14,15]. Antioxidant potential also were tested for Artepillin C derivatives, which displayed remarkable enhancement of scavenging radical activities [16]. Meanwhile, an interestingly particular feature of tumor cells is the acidic extracellular matrix resulting from the lactate production through the anaerobic glycolytic pathway for energy generation of the cells [13,17]. The low pH of extracellular matrix may change the protonation state of pH-dependent bioactive compounds, such as Artepillin C, probably modulating its action to damage the cellular membrane of tumor cells, as known for other compounds [13].

The biological characteristics above described motivated us to investigate the molecular properties of Artepillin C on aqueous solution, since most of biological molecules are embedded in fluids, especially water. This study was performed by optical absorption, steady state and time-resolved fluorescence spectroscopies, which are powerful and sensitive techniques to evaluate the protonation state, the aggregation state and the hydrophobic-hydrophilic characteristics of many natural compounds [18].

2. Material and Methods

2.1. Material

Artepillin C, isolated and purified (98.43%) from green propolis, was purchased from Apis Flora (Ribeirão Preto, SP, Brazil). Phosphate, citric acid and methanol of analytical grade were obtained from Sigma Chemical Co. (St. Louis, MO, USA). Aqueous solutions were prepared with ultrapure Milli-Q® water.

2.2. Optical Absorption and Fluorescence Measurements

Firstly, in acid-base titration experiments, citrate (0.1 M, pH 2.6) and phosphate (0.2 M, pH 9.2) buffers were prepared and, from a citrate-phosphate mixture, 25 samples were obtained with pH value in the
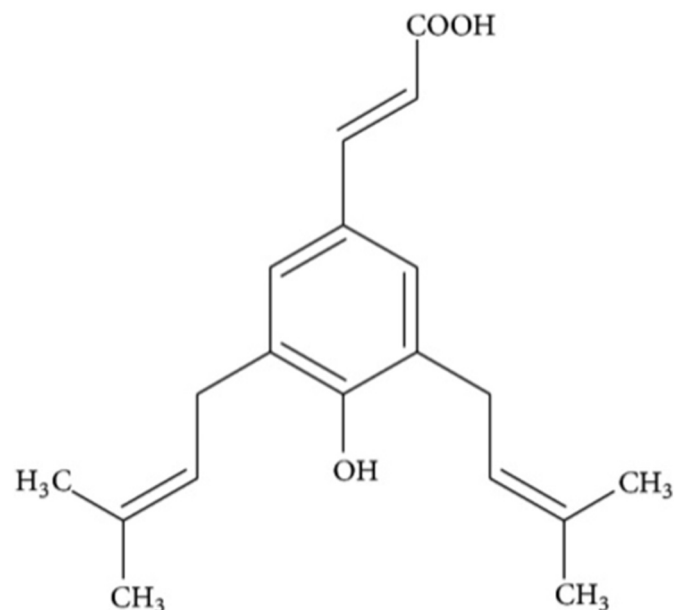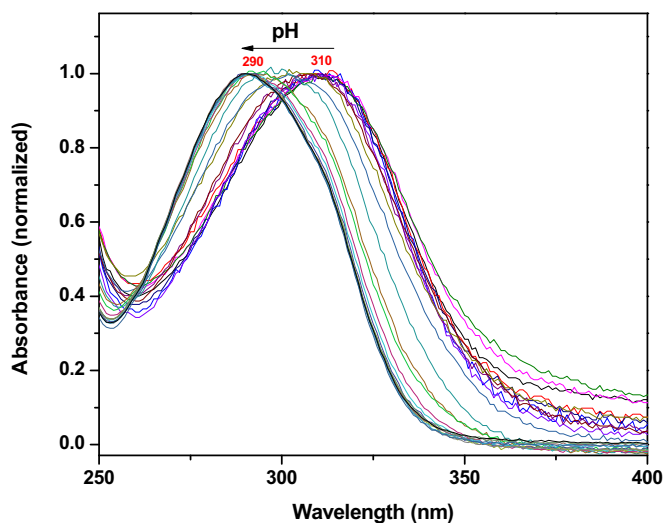

Fig. 2. Optical absorption spectra of Artepillin C 20 μM measured in the pH range 2.6 to 9.2. Spectra normalized in the maximum intensity of the absorption band. Temperature 25 °C.

interval 2.6 to 9.2. An aliquot from a stock solution of Artepillin C in methanol (30 mM) was injected into each citrate-phosphate buffer solution, so that the concentration of the compound was 20 μM in the samples at different pH values. From optical absorption spectra, a titration curve was obtained and the pKa for Artepillin C was determined. The influence of pH and concentration of Artepillin C on the optical absorption and emission properties of the compound were investigated by preparing solutions with concentrations of Artepillin C ranging from 10 to 100 μM in citrate-phosphate buffer at pH 3.0, 4.9 and 7.0.

Optical absorption spectra were obtained with an Amersahmical-Pharmacia Ultrospec 2100 pro spectrophotometer. A Hitachi F-7000 spectrofluorimeter, with polarizer filters for anisotropy experiments, was used for steady state fluorescence measurements. Fluorescence decays and time-resolved anisotropy were measured using single photon counting method. The excitation source was a Tsunami 3950 Spectra Physics titanium-sapphire laser, pumped by a Millennia X Spectra Physics solid state laser. The repetition rate of the pulses was set to 8.0 MHz using the 3980 Spectra Physics pulse picker. The laser was tuned so that a third harmonic generator BBO crystal (GWN-23PL Spectra Physics) gave the 296 nm excitation pulses that were directed to an Edinburgh
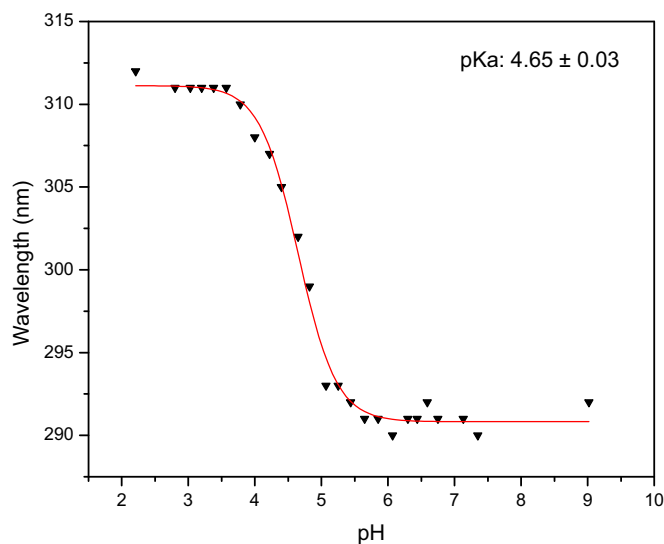

Fig. 1. Molecular structure of Artepillin C.

Fig. 3. Titration curve for Artepillin C: wavelength of the peak of the near UV absorption band, as a function of the pH of the medium. Concentration of Artepillin C 20 μM.
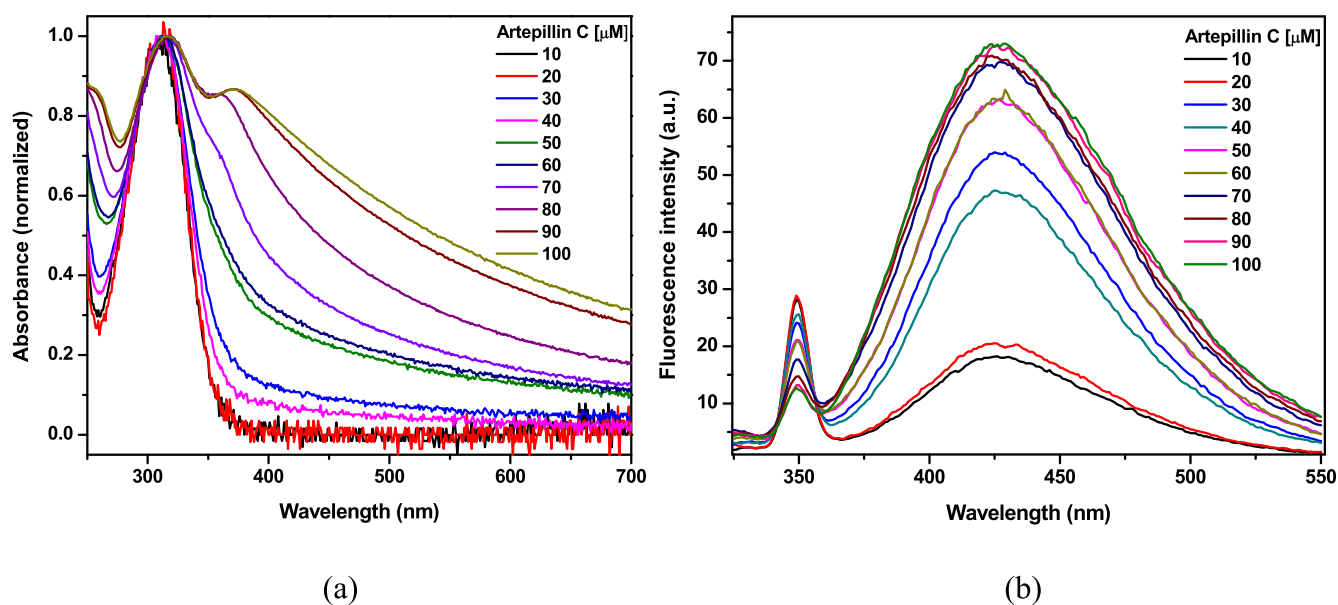
(a)   (b)

Fig. 4. a) Normalized optical absorption spectra of Artepillin C at different concentrations in citrate-phosphate buffer, pH 3.0. b) Fluorescence emission spectra of Artepillin C at different concentrations in citrate-phosphate buffer, pH 3.0, excitation at 310 nm. Temperature 25 °C.

FL900 spectrometer. The spectrometer was set in L-format configuration, the emission wavelength was selected by a monochromator, and emitted photons were detected by a refrigerated Hamamatsu R3809U microchannel plate photomultiplier. Soleil-Babinet compensator in the excitation beam and Glann-Thomson polarizer in the emission beam were used in anisotropy experiments. The FWHM of the instrument response function was typically 100 ps and time resolution was 12 ps per channel and the software provided by Edinburgh Instruments was used to analyze the individual decays, which were fitted to multi-exponential curves.

$$I(t) = \sum \alpha_i e^{(-t/\tau_i)} \qquad (1)$$

where α_i and τ_i are, respectively, pre-exponential factor and lifetime of the component i of decay. The quality of the fit was judged by the

analysis of the statistical parameter reduced-χ^2 and by inspection of the residuals distribution.

3. Results and Discussion

3.1. pH Effects: Determination of pKa

Samples of Artepillin C were prepared in low concentration, 20 μM, and optical absorption spectra were measured in the pH range 2.6 to 9.2. At that concentration each spectrum was dominated by a main absorption band in the near UV region, whose peak displaced from 310 to 290 nm with the increase in pH (Fig. 2, peak normalized absorption spectra).

We expected that at such low concentration the changes in the acid-base equilibrium of the compound were the relevant factor associated to the changes in the main absorption band, and the shift in the
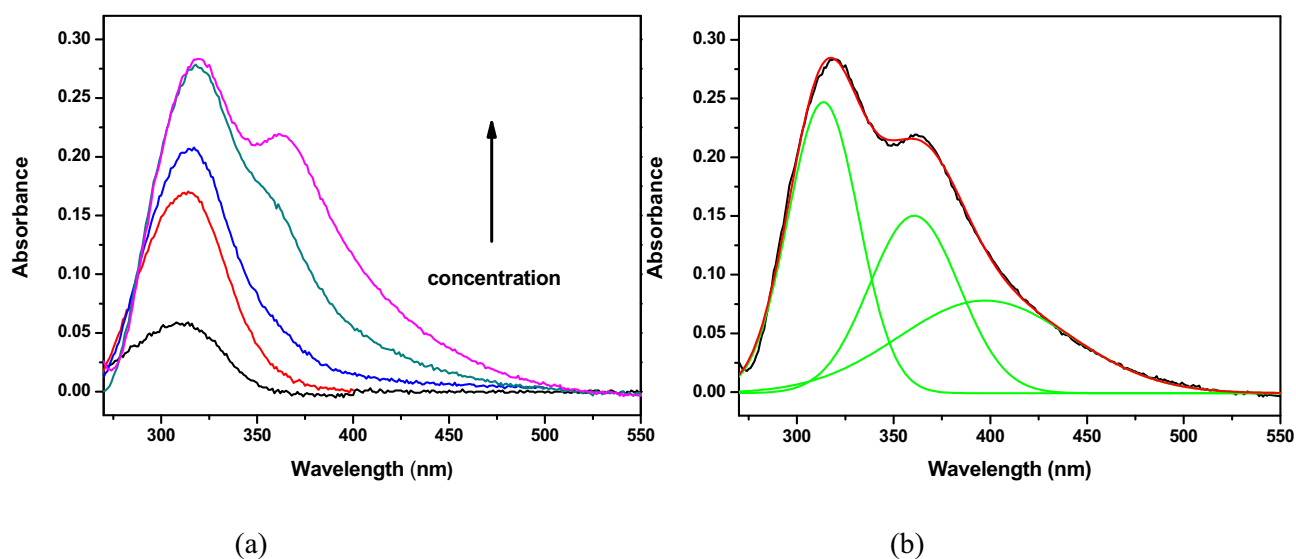

(a)   (b)

Fig. 5. a) Optical absorption spectra corrected by subtraction of baseline for Artepillin C at different concentrations (from below, 10, 30, 50, 70, 80 μM) in citrate-phosphate buffer, pH 3.0. b) Fit (red) of Gaussian curves (green) to the spectrum (black) of Artepillin C 80 μM.
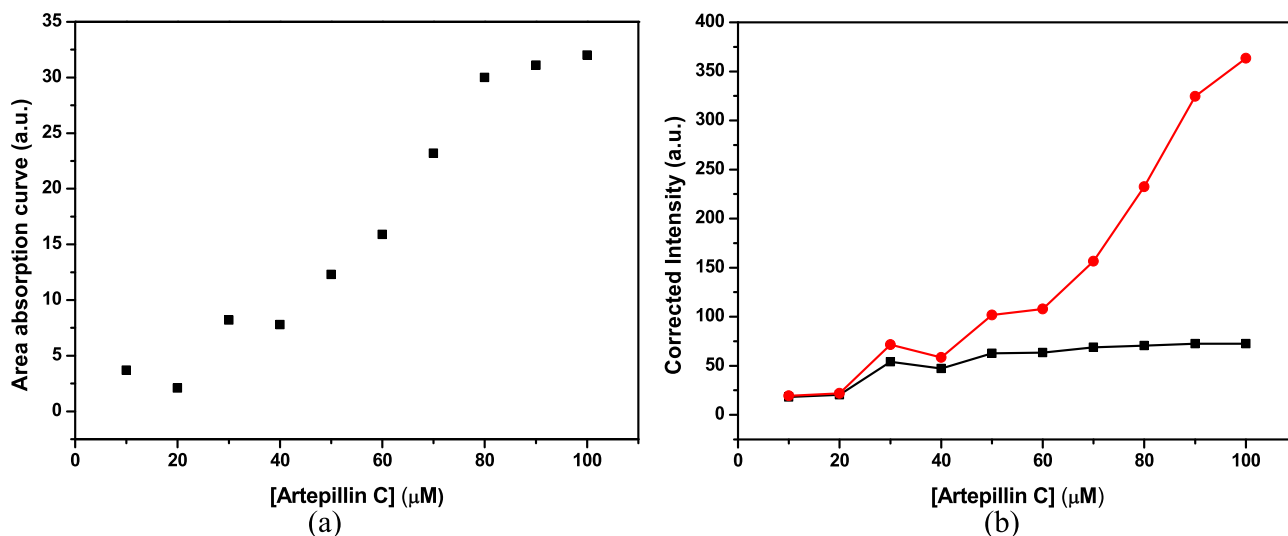
Fig. 6. a) Change in the integrated area under the corrected absorption spectrum with increase in the Artepillin C concentration, in citrate-phosphate buffer pH 3.0. (b) Lower curve (black), intensity of fluorescence emission of Artepillin C at 425 nm, in different concentrations in citrate-phosphate buffer, pH 3.0. Upper curve (red), intensity corrected for absorbance at excitation and emission wavelength.

maximum wavelength of the absorption band reflects the changes in the protonation state of the carboxylic group. A titration curve, given by the plot of the wavelength of the absorption peak as function of pH allows the determination of the pKa of Artepillin C by finding the point of inflection of the fitted curve (Fig. 3). The value obtained was 4.65 ± 0.03, corresponding to the equilibrium between protonated and deprotonated forms of the carboxyl group of Artepillin C (Fig. 1).

Concomitant to changes in the peak position, the absorbance of Artepillin C raised with increase in the pH of the solution. The calculated molar absorption coefficient changed from $0.61 \times 10^4 \, M^{-1} \, cm^{-1}$ at acidic pH, below pH 4.0, to $2.13 \times 10^4 \, M^{-1} \, cm^{-1}$ in neutral pH. The neutral protonated form of Artepillin C, dominant when the pH of the medium is below 4.65, has emission with the near UV band peaking at 305 nm, and low molar absorption coefficient. The deprotonated form, dominant in pH values above 4.65, possess a negative charge in the carboxyl group, and has the near UV absorption band displaced to 290 nm, with increased molar absorption coefficient compared to the neutral species. The results suggest that in deprotonated Artepillin C the electronic distribution is more delocalized and less structured than in the

protonated or neutral species. This affects the magnitude of the static dipole moment in the ground and excited state, resulting in a blue-shift of the electronic absorption band as described for molecular complexes functionalized with carboxylic acid [19], and also for organic compounds like *ortho*-aminobenzoic acid and derivatives [20–22].

3.2. Concentration Effects in Different pHs: Aggregation of Artepillin C

The influence of concentration in the spectroscopic properties of Artepillin C was examined in three different pHs separately. We assumed that in pH values below (3.0) and above (7.0) the pKa of Artepillin C, the compound is predominantly in neutral and anionic forms respectively. and at pH around the pKa both species are present.

3.2.1. pH 3.0: Protonated Artepillin C
Optical absorption spectra in citrate-phosphate buffer pH 3.0 were obtained at Artepillin C concentrations in the range 10 to 100 μM (Fig. 4a). The absorption band centered around 315 nm is present in all concentrations, and above 50 μM of Artepillin C, a new band appears
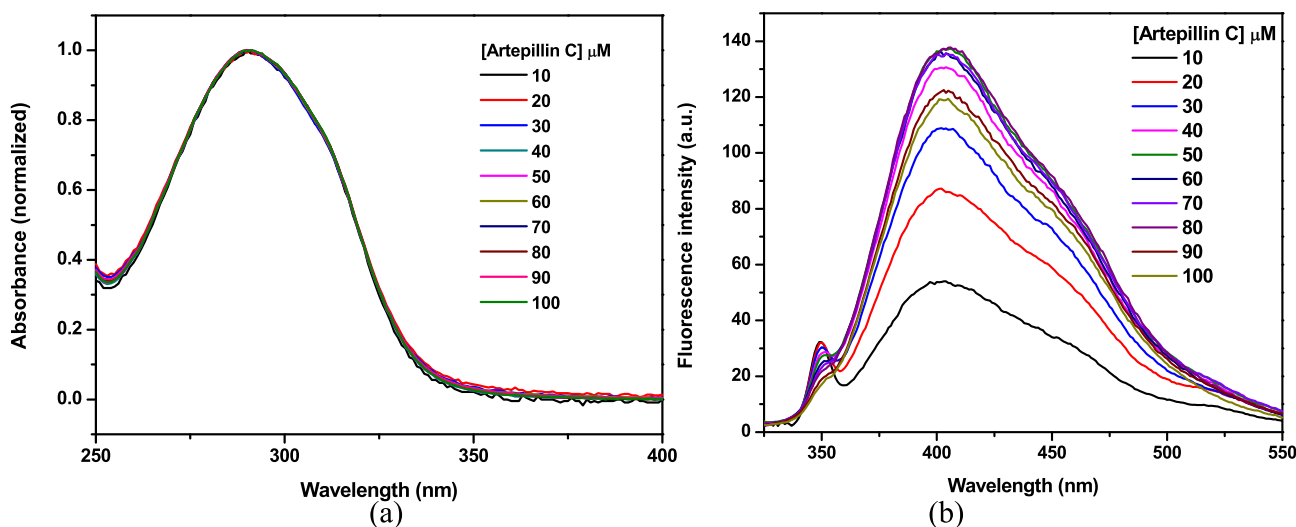

Fig. 7. a) Optical absorption spectra of Artepillin C in citrate-phosphate buffer, pH 7.0. b) Fluorescence spectra of Artepillin C in citrate-phosphate buffer, pH 7.0, excitation 310 nm. Temperature 25 °C.
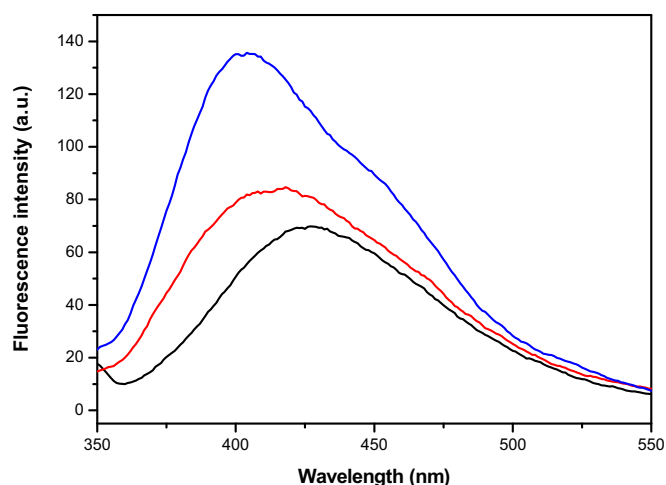
Fig. 8. Emission spectra of Artepillin C 80 μM in pH 3.0 (black), 4.9 (red) and 7.0 (blue). Excitation wavelength 310 nm. Temperature 25 °C.

around 360 nm, whose intensity increases at higher concentrations. Fluorescence emission spectra of Artepillin C in concentrations between 10 and 100 μM in citrate-phosphate buffer pH 3.0 were recorded with excitation at 310 nm, showing emission around 425 nm (Fig. 4b).

The changes in the absorption spectra are better visualized performing baseline subtraction in the spectra (Fig. 5a). It is clearly seen that in concentrations above 50 μM a band at wavelength above 350 nm becomes discernible, and the spectra broadens at higher concentrations of Artepillin C, above 70 μM. The corrected spectra can be fitted to gaussians bands and for the lower concentrations, below 30 μM, one gaussian centered around 312 nm is enough to fit the spectra. At intermediate concentrations (40–60 μM) appears the contribution of a second gaussian centered around 347 nm. In still higher concentrations, a third broad gaussian, centered above 400 nm contributes to the spectra (in Fig. 5b, illustration of the fit to three gaussians performed to the spectrum of Artepillin C 80 μM; more details can be seen in Supporting Material 1).

As described above, the carboxyl group is protonated and the molecule is in the electrically neutral state. As the molecules are in neutral state, it is possible that they aggregate, due to hydrophobic interactions [22]. The species formed can be in the form of J-aggregates, expressed by

the longer wavelength (around 350 nm) in the absorption band [23] An approximately linear increase in the area under the absorption spectrum is observed for concentrations below 60 μM (Fig. 6a). Above that concentration, aggregated species increase the cross section for absorption, with corresponding increase in the area under the absorption spectrum.

Under excitation at 310 nm, the emission spectrum of Artepillin C is characterized by a broad emission centered around 425 nm independent of its concentration (Fig. 4b). The intensity of emission does not increase linearly with the concentration due to inner filter effects caused by the high absorbance of the more concentrated samples (Fig. 6b). As the more concentrated solutions present high absorbance both at excitation and emission wavelengths, inner filter effects become appreciable. The corrections for inner filter attenuation applied to the emission intensity, leads to the expected increase of emission with increase in the concentration of Artepillin C.

3.2.2. pH 7.0: Deprotonated Artepillin C

At neutral pH, optical absorption spectra of Artepillin C in the concentration range 10 to 100 μM show the near UV absorption band centered at 291 nm, corresponding to the deprotonated and negatively charged form of the molecule (Fig. 7a). The absorbance at the peak follows the Beer-Lambert law, with linear increase with the concentration of Artepillin C (Supporting Material 2).

The fluorescence emission spectra were obtained with excitation at 310 nm. The spectra are quite broad, with maximum emission around 400 nm. The intensities do not increase linearly with the concentration, because the measurements are affected by the high extinction coefficient of the absorption at the excitation wavelength. Intensities corrected for inner filter effects showed an upward deviation from linearity. A comparison for the emission spectra at different pHs, with excitation at 310 nm, is illustrated in Fig. 8. Similar to the absorption spectra, the spectral position of the emission band depends on the pH of medium: the wavelength for maximum emission locates at 425 nm in the protonated form of Artepillin C (pH 3.0); close to the pKa, the maximum emission occurs at 410 nm (pH 4.9); and for the deprotonated species of Artepillin C, the emission peaks in 400 nm (pH 7.0). The blue-shift observed in fluorescence emission spectra from protonated to deprotonated is also related to the delocalized and less structured electronic transition in deprotonated compounds, as discussed for the absorption spectra of Artepillin C.

At pH 7.0, it is noticeable the appearance of a broad red shifted band with emission above 450 nm. One possibility for this long wavelength

(a)   (b)
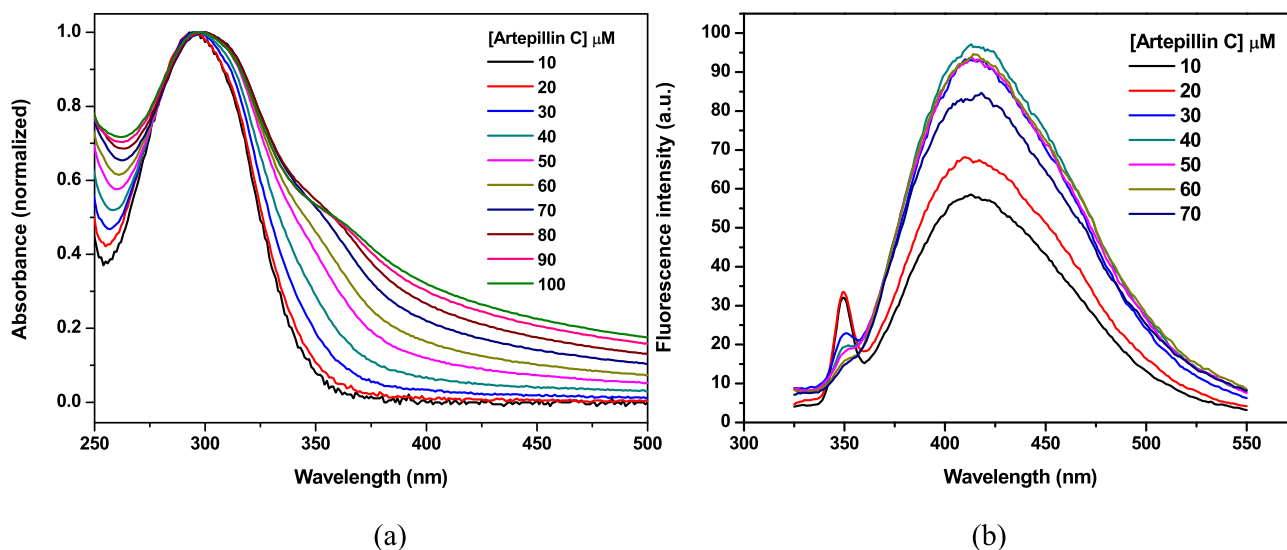
Fig. 9. a) Optical absorption spectra of Artepillin C in citrate-phosphate buffer pH 4.9. b) Fluorescence spectra of Artepillin C in citrate-phosphate buffer pH 4.9, excitation 310 nm. Temperature 25 °C.
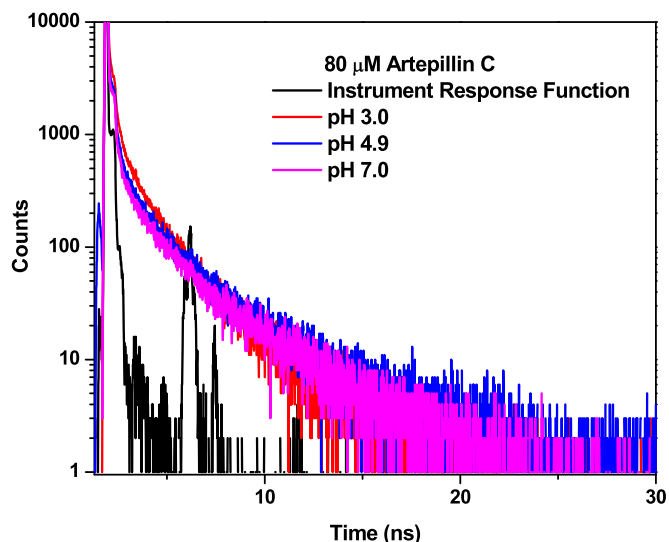
Fig. 10. Intensity decay profiles of Artepillin C 80 μM, at pH 3.0 (red), 4.9 (blue) and 7.0 (pink). Excitation 296 nm, emission 400 nm, temperature 25 °C. The black curve represents the Instrument Response Function (IRF).

emission is the occurrence of isomeric forms of deprotonated anionic Artepillin C. Different isomeric forms involving the carboxy group result in distinct interactions with the proton donor water molecules, as observed for example in ortho-aminobenzoic or anthranilic acid molecules, both experimentally as in electronic structure calculations [20,24]. Due to different solvent relaxation processes for the excited state of the transition dipoles from the isomers, the emission wavelength may be different, with the occurrence of dual emission [22,25]. In low pH, the neutral protonated isomers should have similar interactions via hydrogen bonds with the water molecules.

3.2.3. pH 4.9: Protonated and Deprotonated Species

At this pH, Artepillin C is close to the equilibrium between protonated and deprotonated species. The optical absorption spectra are broad and have maximum around 296 nm, with a noticeable contribution from a band with maximum around 310 nm (Fig. 9a). Compared to the spectra obtained for the titration curve, the data indicate the coexistence of both protonated and deprotonated forms of the carboxy group in Artepillin C. At low concentration, 20 μM, absorption spectrum can be fitted to two gaussians, one centered at 293 nm with height 0.98 and the other at 313 nm, with height 0.09. The spectrum is dominated by the deprotonated species because of its higher molar absorptivity (2.13×10^4 M^{-1} cm^{-1}) compared to the protonated form (0.61×10^4 M^{-1} cm^{-1}). On the other hand, at high Artepillin C concentration, 100 μM, the absorbance is fitted with three gaussians centered at 298, 318 and 334 nm, with heights 0.42, 0.42 and 0.45 respectively and we can observe the contribution of a broad band at longer wavelength, indicating that probably aggregates are formed involving the protonated forms of Artepillin C, present at pH 4.9. Fitting parameters for optical absorption spectra of 20 and 100 μM of Artepillin C can be found at Supporting Material 3.

Fluorescence emission spectra were obtained exciting the samples at 310 nm (Fig. 7b). The spectra are relatively broad, with maximum emission around 410 nm. The intensities do not increase linearly with the concentration, because the measurements are affected by the high extinction coefficient of the absorption at the excitation wavelength.

3.3. Fluorescence Intensity and Anisotropy Time-resolved Decay

In time-resolved experiments, samples containing 20 μM or 80 μM of Artepillin C in the pH 3.0, 4.9 and 7.0 were excited with pulsed laser tuned at 296 nm. The intensity decay was complex, and decay profiles required three-exponential curves for adequate fit (Fig. 10 and Table 1). The component associated to the short lifetime, around 50 ps, is predominant, showing the highest value of the normalized pre-exponential factor. Intermediate lifetimes around 0.60–0.80 ns were also present, and best fit was obtained with inclusion of a very small contribution of a long lifetime components higher than 2.0 ns.

Average lifetimes were calculated using

$$<\tau> = \frac{\sum \alpha_i \tau_i^2}{\sum \alpha_i \tau_i} \tag{2}$$

obtained from the usual definition of average applied to Eq. (1) and the calculated values are in the hundred-picosecond region, showing that very efficient non-radiative processes dominate the decay from the excited state.

Steady state anisotropy was measured in pH 3.0, 4.9 and 7.0 and the values obtained are relatively high: 0.209, 0.163 and 0.201 for 20 μM and 0.189, 0.253 and 0.199 for 80 μM of Artepillin C, respectively. The results must consider that steady state anisotropy depends on both intensity decay and anisotropy decay [18]. On the above pHs, the rotational correlation times for the anisotropy decay were 0.445, 0.461 and 0.590 ns for 20 μM and 0.541, 0.728 and 0.645 ns for 80 μM of Artepillin C, respectively. As the dominant lifetime values are very short (Table 1), the excited state is depopulated before the emission dipoles perform rotational diffusion. Therefore, the emission occurs much before the fluorophores rotate, and the value of the intensity component perpendicular to the direction of excitation is small, resulting in high values for the steady state anisotropy. From the time-resolved data it was possible to calculate a mean value for the anisotropy [26], resulting in values between 0.13 and 0.28 (Table 2).

4. Conclusions

Optical absorption and fluorescence spectroscopies allowed the identification of different molecular arrangements of Artepillin C, the major component of green propolis, in aqueous solutions at different pHs. The compound is derived from cinnamic acid, presenting a carboxyl group susceptible to protonation-deprotonation processes. In conditions of low concentration, acid-base titration monitoring the spectral position of the near UV absorption band, resulted in the pKa value of 4.65 for the carboxylic group in Artepillin C.

Concentration effects observed in optical absorption spectra were dependent on the pH of the medium. In acidic pH, below the pKa value, an absorption band raised around 350 nm when the Artepillin C concentration was higher than 50 μM. As the compound at that pH is

Table 1
Intensity decay parameters for Artepillin C in citrate-phosphate buffer, pH 3.0, 4.9 and 7.0; emission wavelength at 400 nm. Temperature 25 °C.

pH - Citrate-phosphate buffer	Artepillin C concentration (μM)	τ_1 (ns)	α_1	τ_2 (ns)	α_2	τ_3 (ns)	α_3	$<\tau>$
3.0	20	0.051	0.940	0.60	0.054	3.45	0.0034	0.46
4.9		0.066	0.970	0.66	0.026	3.42	0.0052	0.62
7.0		0.058	0.980	0.8	0.017	3.2	0.0012	0.18
3.0	80	0.036	0.984	0.54	0.014	2.01	0.0020	0.20
4.9		0.032	0.993	0.81	0.006	4.05	0.0006	0.26
7.0		0.028	0.996	0.89	0.004	4.18	0.0004	0.20

Table 2
Steady state anisotropy (A_S), rotational correlation time (φ), initial anisotropy (B) and calculated average anisotropy <A>.

pH - Citrate-phosphate buffer	Artepillin C concentration (μM)	A_s	φ (ns)	B	<A>
3.0	20	0.209	0.445	0.396	0.169
4.9		0.163	0.461	0.356	0.205
7.0		0.201	0.590	0.372	0.262
3.0	80	0.189	0.541	0.224	0.127
4.9		0.253	0.728	0.336	0.213
7.0		0.199	0.645	0.352	0.283

electrically neutral, aggregation could be occurring, resulting in the rising of long wavelength absorption band. In pH 4.9, there must be an equilibrium between protonated and deprotonated species, that coexists contributing to the spectral characteristics of the compound. In neutral pH the deprotonated negatively charged form of Artepillin C dominates, which absorbs at 290 nm and emits with maximum at 400 nm. It is possible that isomeric forms are present in the solution, with different interaction with the aqueous environment and distinct relaxation processes, leading to dual emission at 400 and 450 nm.

Intensity decays at the different pHs were fitted to three exponential function. The decay was fast, dominated by a very short lifetime component, around 0.060 ns. The fast decay precluded the rotational diffusion of the excited transition dipole, and emission occurs before fluorescence depolarization, resulting in values of the fluorescence anisotropy higher than could be expected for monomeric forms of the compound.

Artepillin C is known by the affinity with amphiphilic aggregates, in processes that can be relevant to its biological activity. The results described here points to the importance of the knowledge of the protonation state of the molecule, that can be relevant in processes mediated by biological membranes. As a first systematic compilation of spectroscopic data of Artepillin C, there still remain important questions deserving attention, like the influence of isomerization in the optical properties of the molecule. We believe that further studies including, e.g., electronic structure calculations and molecular dynamics simulations could be helpful to improve the understanding of the absorption and emission properties of Artepillin C.

Acknowledgements

Conflicts of interest

None.

Appendix A. Supplementary data

Supplementary data to this article can be found online at https://doi.org/10.1016/j.saa.2018.02.059.

References

[1] J.M. Sforcin, Propolis and the immune system: a review, J. Ethnopharmacol. 113 (2007) 1–14, https://doi.org/10.1016/j.jep.2007.05.012.
[2] J.F. Campos, U.P. dos Santos, P. dos S. da Rocha, M.J. Damião, J.B.P. Balestieri, C.A.L. Cardoso, E.J. Paredes-Gamero, L.M. Estevinho, K. de Picoli Souza, E.L. dos Santos, Antimicrobial, antioxidant, anti-inflammatory, and cytotoxic activities of propolis from the stingless bee *Tetragonisca fiebrigi* (Jataí), Evidence-Based Complement. Altern. Med. 2015 (2015) 1–11, https://doi.org/10.1155/2015/296186.
[3] J.M. Sforcin, V. Bankova, Propolis: is there a potential for the development of new drugs? J. Ethnopharmacol. 133 (2011) 253–260, https://doi.org/10.1016/j.jep.2010.10.032.
[4] A. Salatino, C.C. Fernandes-Silva, A.A. Righi, M.L.F. Salatino, Propolis research and the chemistry of plant products, Nat. Prod. Rep. 28 (2011) 925, https://doi.org/10.1039/c0np00072h.
[5] A.C.H.F. Sawaya, I.B.S.C, M.C. Marcucci, Analytical methods applied to diverse types of Brazilian propolis, Chem. Cent. J. 5 (2011) 27, https://doi.org/10.1186/1752-153X-5-27.
[6] M.-R. Ahn, K. Kunimasa, T. Ohta, S. Kumazawa, M. Kamihira, K. Kaji, Y. Uto, H. Hori, H. Nagasawa, T. Nakayama, Suppression of tumor-induced angiogenesis by Brazilian propolis: major component artepillin C inhibits in vitro tube formation and endothelial cell proliferation, Cancer Lett. 252 (2007) 235–243, https://doi.org/10.1016/j.canlet.2006.12.039.
[7] S. Kumazawa, T. Hamasaka, T. Nakayama, Antioxidant activity of propolis of various geographic origins, Food Chem. 84 (2004) 329–339, https://doi.org/10.1016/S0308-8146(03)00216-4.
[8] H. Aga, T. Shibuya, T. Sugimoto, Isolation and identification of antimicrobial compounds in Brazilian propolis, Biosci. Biotechnol. Biochem. 58 (1994) 945–946, https://doi.org/10.1080/bbb.58.945.
[9] M.C. Marcucci, F. Ferreres, C. García-Viguera, V.S. Bankova, S.L. de Castro, A.P. Dantas, P.H.M. Valente, N. Paulino, Phenolic compounds from Brazilian propolis with pharmacological activities, J. Ethanopharmacol. 74 (2001) 105–112.
[10] W.M. Pazin, L. da M. Mônaco, A.E. Egea Soares, F.G. Miguel, A.A. Berretta, A.S. Ito, Antioxidant activities of three stingless bee propolis and green propolis types, J. Apic. Res. 56 (2017) 40–49, https://doi.org/10.1080/00218839.2016.1263496.
[11] H. Hattori, K. Okuda, T. Murase, Y. Shigetsura, K. Narise, G.L. Semenza, H. Nagasawa, Isolation, identification, and biological evaluation of HIF-1-modulating compounds from Brazilian green propolis, Bioorg. Med. Chem. 19 (2011) 5392–5401, https://doi.org/10.1016/j.bmc.2011.07.060.
[12] W.M. Pazin, D. da S. Olivier, N. Vilanova, A.P. Ramos, I.K. Voets, A.E.E. Soares, A.S. Ito, Interaction of artepillin C with model membranes, Eur. Biophys. J. 46 (2017) 383–393, https://doi.org/10.1007/s00249-016-1183-5.
[13] Y. Kato, S. Ozawa, C. Miyamoto, Y. Maehata, A. Suzuki, T. Maeda, Y. Baba, Acidic extracellular microenvironment and cancer, Cancer Cell Int. 13 (2013) 89, https://doi.org/10.1186/1475-2867-13-89.
[14] Y. Uto, S. Ae, D. Koyama, M. Sakakibara, N. Otomo, M. Otsuki, H. Nagasawa, K.L. Kirk, H. Hori, Artepillin C isoprenomics: design and synthesis of artepillin C isoprene analogues as lipid peroxidation inhibitor having low mitochondrial toxicity, Bioorg. Med. Chem. 14 (2006) 5721–5728, https://doi.org/10.1016/j.bmc.2006.04.015.
[15] I. Nakanishi, Y. Uto, K. Ohkubo, K. Miyazaki, H. Yakumaru, S. Urano, H. Okuda, J.I. Ueda, T. Ozawa, K. Fukuhara, S. Fukuzumi, J. Nagasawa, H. Hori, N. Ikota, Efficient radical scavenging ability of artepillin C, a major component of Brazilian propolis, and the mechanism, Org. Biomol. Chem. 1 (2003) 1452–1454, https://doi.org/10.1039/B302098c.
[16] S. Manda, I. Nakanishi, K. Ohkubo, Y. Uto, T. Kawashima, H. Hori, K. Fukuhara, H. Okuda, T. Ozawa, N. Ikota, S. Fukuzumi, K. Anzai, Enhanced radical-scavenging activity of naturally-oriented artepillin C derivatives, Chem. Commun. (Camb.) (2008) 626–628, https://doi.org/10.1039/b715973k.
[17] S.R. McKeown, Defining normoxia, physoxia and hypoxia in tumours—implications for treatment response, Br. J. Radiol. 87 (2014), 20130676. https://doi.org/10.1259/bjr.20130676.
[18] L.S. Berlim, A.G. Bezerra, W.M. Pazin, T.S. Ramin, W.H. Schreiner, A.S. Ito, Photophysical properties of flavonoids extracted from *Syngonanthus nitens*, the golden grass, J. Lumin. 194 (2018) 394–400, https://doi.org/10.1016/j.jlumin.2017.10.040.
[19] E. Badaeva, V.V. Albert, S. Kilina, A. Koposov, M. Sykora, S. Tretiak, Effect of deprotonation on absorption and emission spectra of Ru(II)-bpy complexes functionalized with carboxyl groups, Phys. Chem. Chem. Phys. 12 (2010) 8902–8913, https://doi.org/10.1039/b924910a.
[20] M. Takara, A.S. Ito, General and specific solvent effects in optical spectra of ortho-aminobenzoic acid, J. Fluoresc. 15 (2005) 171–177, https://doi.org/10.1007/s10895-005-2525-3.
[21] M. Takara, J.K. Eisenhut, I.Y. Hirata, L. Juliano, A.S. Ito, Solvent effects in optical spectra of ortho-aminobenzoic acid derivatives, J. Fluoresc. 19 (2009) 1053–1060, https://doi.org/10.1007/s10895-009-0505-8.
[22] C.A. Marquezin, I.Y. Hirata, L. Juliano, A.S. Ito, Spectroscopic characterization of 2-amino-N-hexadecyl-benzamide (AHBA), a new fluorescence probe for membranes, Biophys. Chem. 124 (2006) 125–133, https://doi.org/10.1016/j.bpc.2006.06.002.
[23] L.P.F. Aggarwal, I.E. Borissevitch, On the dynamics of the TPPS4 aggregation in aqueous solutions: successive formation of H and J aggregates, Spectrochim. Acta - Part A Mol. Biomol. Spectrosc. 63 (2006) 227–233, https://doi.org/10.1016/j.saa.2005.05.009.
[24] D. da S. Olivier, A.S. Ito, S.E. Galembeck, Microhydration effects on geometric properties and electronic absorption spectra of ortho-aminobenzoic acid, Spectrochim. Acta Part A Mol. Biomol. Spectrosc. 147 (2015) 328–333, https://doi.org/10.1016/j.saa.2015.03.108.
[25] A. Amat, C. Clementi, F. De Angelis, A. Sgamellotti, S. Fantacci, Absorption and emission of the apigenin and luteolin flavonoids: a TDDFT investigation †, J. Phys. Chem. A 113 (2009) 15118–15126, https://doi.org/10.1021/jp9052538.
[26] A.S. Ito, A.P. Rodrigues, W.M. Pazin, M.B. Barioni, Fluorescence depolarization analysis of thermal phase transition in DPPC and DMPG aqueous dispersions, J. Lumin. (2015)https://doi.org/10.1016/j.jlumin.2014.09.051.